Proceedings of the
2007 IEEE Intelligent Vehicles Symposium
Istanbul, Turkey, June 13-15, 2007

Short Range Radar Signal Processing for Lateral Collision Warning in Road Traffic Scenarios

Dirk Bank, *Member, IEEE*

***Abstract*—This paper introduces signal processing algorithms of single-sensor-multi-target-tracking, sensor data fusion, and multi-sensor-multi-target-tracking developed for designing a novel lateral collision warning function. In order to improve the perception of road vehicles, an experimental vehicle has been equipped with arrays of three short range radar sensors on both sides. With the aid of such sensor arrangements, lateral objects (e.g. cars, trucks, bicycles, guard rails) can be detected and tracked. Thus, imminent collisions in the lateral area may be prevented by warning the driver when the ego-vehicle inadvertently drifts towards another vehicle on the adjacent lane or towards the road boundary, or when another vehicle approaches the ego-vehicle in a dangerous manner.**

I. Introduction

There is a strong believe that the improvement of preventive safety applications and the extension of their operative range will be achieved by the deployment of multiple sensors with wide fields of view [18]. This paper presents dedicated signal processing algorithms for the implementation of a lateral collision warning (LCW) function based on wide-angled short range radar (SRR) sensors as a contribution to the enhancement of active safety in road traffic scenarios.

For state estimation and target tracking, the Kalman Filter [13, 14] is employed. Maybeck [17] provides a detailed insight into the subject of stochastic models, estimation, and control. Major contributions to tracking originate from Bar-Shalom and his associates [1, 2, 3, 4, 5, 6]. Blackman [7] covers multiple-target-tracking with radar applications, and Blackman and Popoli [8] address the design and analysis of modern tracking systems. Lerro and Bar-Shalom [16] present a comparison between tracking with debiased consistent converted measurements and the extended Kalman Filter. Hall and Llinas [10] edited an handbook of multi-sensor data fusion. As a new extension of the Kalman Filter to nonlinear systems, the unscented transform was introduced by Julier and Uhlmann [11, 12]. Lefebvre et al. [15] compare the performance of different Kalman Filters for nonlinear systems.

The content of this paper is organized as follows. A short description of the employed SRR sensors is contained in Section II, and the development of a sensor model is explained in Section III. The algorithms of single-sensor-multi-target-tracking, sensor data fusion, and multi-sensor-multi-target-tracking are established in Section IV, Section V, and Section VI. Experimental results are presented in Section VII, and a conclusion is provided in Section VIII.

Manuscript received December 14, 2006. This work was supported in part by the European Commission under the project PReVENT, subproject Lateral Safe.

D. Bank is with the Environment Recognition Department, DaimlerChrysler Research and Technology, 89081 Ulm, Germany (phone: +49-(0)731-505-2276; fax: +49-(0)731-505-4105; e-mail: dirk.bank@daimlerchrysler.com).

II. Short Range Radar Sensor

SRR signal processing is based on sensor arrays installed on both sides of the vehicle. For this purpose, three sensors are placed at each side with distances of 0.5m, 2.0m, and 4.0m from the front of the car. The sensors are orientated perpendicular to the side of the car. Figure 1 shows the locations of the coordinate systems used for SRR signal processing.

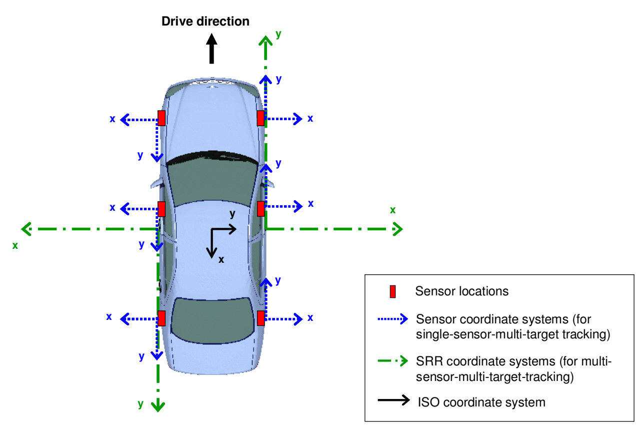

Fig. 1. Locations of the coordinate systems used for SRR signal processing

An exploded view of the employed SRR sensor from M/A-COM / Tyco Electronics [9] is shown in Figure 2.

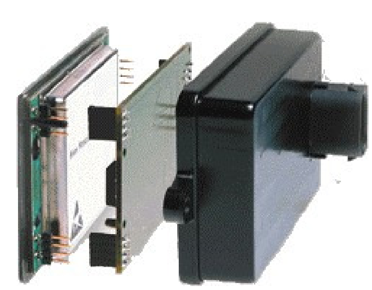

Fig. 2. M/A-COM / Tyco Electronics SRR sensor

Technical characteristics of the SRR sensor:
Frequency: 24.125GHz (Bandwidth: 5GHz)
Detection cycle time: 40ms
Antenna Detection Characteristic (3db limit):
±8° elevation, ±65° azimuth
Number of detectable targets per sensor: 10
Target parameter types: range, bearing, velocity
Distance detection range: 0.2m – 30m
Distance accuracy: 0.075m
Distance resolution (target resolution): 0.15m
Bearing detection range: ±40°
Bearing accuracy (typical):
±5° for bearing range 0° - ±5°
±10° for bearing range ±5° - ±40°

III. Sensor Modeling

A sensor model (see Figure 3 and Figure 4) has been developed which considers distance detection range, distance accuracy, bearing detection range, bearing accuracy (for different bearing ranges) of the employed sensors as well as reflection properties of radar waves.

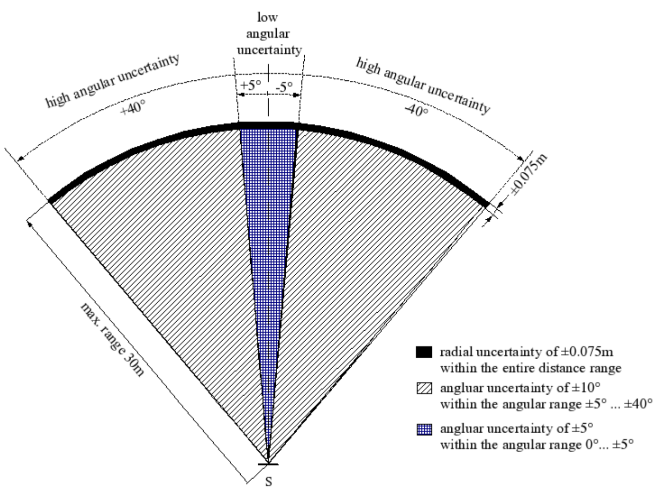

Fig. 3. Sensor model with areas of different angular uncertainty

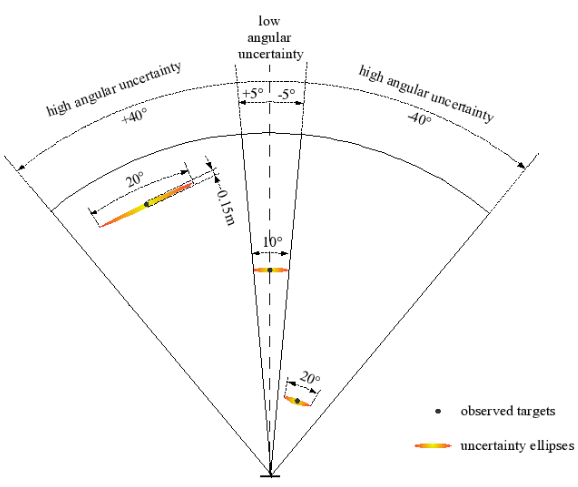

Fig. 4. Sensor model with observed targets and uncertainty ellipses

IV. Single-Sensor-Multi-Target-Tracking

The raw sensor data is filtered and single-sensor-multi-target-tracking is realized for each sensor independently by applying a Mixed Coordinates Kalman Filter (MCKF) and a Converted Measurement Kalman Filter (CMKF) alternatively.

The state and space model of the system is given in Subsection *A*. The required matrices and vectors for the MCKF and CMKF are provided in Subsection *B* and Subsection *C*. A comparison of the alternative Kalman Filter approaches follows in Subsection *D*. Data association is explained in Subsection *E*, and ego-motion-compensation is described in Subsection *F*.

A. State and Space Model

The state vector $\mathbf{x}$ contains the relative target position in Cartesian sensor coordinates (x, y) as well as the relative target velocities in *x*- and *y*-direction (v_x , v_y):

$$\mathbf{x} = \begin{pmatrix} x \\ v_x \\ y \\ v_y \end{pmatrix} \tag{1}$$

The process matrix $\mathbf{F}$ is used to calculate the predicted state vector at time *k*:

$$\hat{\mathbf{x}}_{k|k-1} = \mathbf{F}_{k-1}\hat{\mathbf{x}}_{k-1|k-1} \tag{2}$$

As it is assumed that the speed remains unchanged within one time cycle, the process matrix $\mathbf{F}$ can be derived from the following equations:

$$x_{k|k-1} = x_{k-1|k-1} + T v_{x,k-1|k-1} \tag{3}$$

$$v_{x,k|k-1} = v_{x,k-1|k-1} \tag{4}$$

$$y_{k|k-1} = y_{k-1|k-1} + T v_{y,k-1|k-1} \tag{5}$$

$$v_{y,k|k-1} = v_{y,k-1|k-1} \tag{6}$$

With *T* being the sample time, this yields the process matrix $\mathbf{F}$:

$$\mathbf{F} = \begin{pmatrix} 1 & T & 0 & 0 \\ 0 & 1 & 0 & 0 \\ 0 & 0 & 1 & T \\ 0 & 0 & 0 & 1 \end{pmatrix} \tag{7}$$

For the implementation of the Kalman Filter, a constant velocity model is chosen. To compensate for the negligence of velocity changes, a process noise is modeled, which is assumed to be zero-mean, white Gaussian with variance σ^2. The process noise covariance matrix $\mathbf{Q}$ expresses the influence of this noise on the overall error:

$$\mathbf{Q} = \begin{pmatrix} \frac{1}{4}T^4 & \frac{1}{2}T^3 & 0 & 0 \\ \frac{1}{2}T^3 & T^2 & 0 & 0 \\ 0 & 0 & \frac{1}{4}T^4 & \frac{1}{2}T^3 \\ 0 & 0 & \frac{1}{2}T^3 & T^2 \end{pmatrix} \cdot E\left[a^2\right] \tag{8}$$

As the deceleration / acceleration of the tracked objects (e.g. other cars) ranges from approximately -10m/s^2 to $+5\text{m/s}^2$, the variance $\sigma_a^2 = E[a^2]$ can be estimated as follows:

$$E[a^2] = \left(\frac{\left|-10\text{m/s}^2\right|}{3} \right)^2 = 11.1\text{m}^2/\text{s}^4 \qquad (9)$$

The threefold radial standard deviation $3\sigma_r$ can be estimated from the given distance accuracy of the sensors:

$$3\sigma_r = 0.075\text{m} \qquad \text{for} \quad 0.2\text{m} \le r < 30\text{m} \qquad (10)$$

Accordingly, the threefold angular standard deviation $3\sigma_\theta$ can be estimated from the given angular accuracy of the sensors:

$$3\sigma_\theta = 5° \cdot \frac{\pi}{180°} \qquad \text{for} \quad 0° \le |\theta| < 5° \qquad (11)$$

$$3\sigma_\theta = 10° \cdot \frac{\pi}{180°} \qquad \text{for} \quad 5° \le |\theta| < 40° \qquad (12)$$

B. Mixed Coordinates Kalman Filter (MCKF)

Since the measurement vector $\mathbf{z}$ is obtained in polar sensor coordinates and the state vector $\mathbf{x}$ is defined in rectangular sensor coordinates, a Mixed Coordinates Kalman Filter can be applied.

The measurement vector $\mathbf{z}$ consists of r and θ:

$$\mathbf{z} = \mathbf{h}(\mathbf{x}) = \begin{pmatrix} r \\ \theta \end{pmatrix} = \begin{pmatrix} \sqrt{x^2 + y^2} \\ \arctan \frac{y}{x} \end{pmatrix} \qquad (13)$$

The measurement covariance matrix $\mathbf{R}$ expresses the inaccuracy of the sensor measurements in polar coordinates. The measurement noise is assumed to be zero-mean, white Gaussian with variance σ^2:

$$\mathbf{R} = \begin{pmatrix} \sigma_r^2 & \sigma_{r\theta}^2 \\ \sigma_{r\theta}^2 & \sigma_\theta^2 \end{pmatrix} = \begin{pmatrix} \sigma_r^2 & 0 \\ 0 & \sigma_\theta^2 \end{pmatrix} \qquad (14)$$

Since the angular uncertainty depends on the angular location of the target, the elements of $\mathbf{R}$ depend on the angular location of the target as well.

The measurement matrix $\mathbf{H}$ relates between the measurement vector and the state vector:

$$\mathbf{H} = \frac{\partial \mathbf{h}(\mathbf{x})}{\partial \mathbf{x}} = \begin{pmatrix} \frac{\partial r}{\partial x} & \frac{\partial r}{\partial v_x} & \frac{\partial r}{\partial y} & \frac{\partial r}{\partial v_y} \\ \frac{\partial \theta}{\partial x} & \frac{\partial \theta}{\partial v_x} & \frac{\partial \theta}{\partial y} & \frac{\partial \theta}{\partial v_y} \end{pmatrix} = \begin{pmatrix} \frac{x}{\sqrt{x^2 + y^2}} & 0 & \frac{y}{\sqrt{x^2 + y^2}} & 0 \\ -\frac{y}{x^2 + y^2} & 0 & \frac{x}{x^2 + y^2} & 0 \end{pmatrix} \qquad (15)$$

C. Converted Measurement Kalman Filter (CMKF)

In order to minimize errors due to the transformation from polar coordinates into rectangular coordinates, a Converted Measurement Kalman Filter as described in [16] can be used.

The measurement vector $\mathbf{z}$ consists of x and y:

$$\mathbf{z} = \mathbf{h}(\mathbf{x}) = \begin{pmatrix} x \\ y \end{pmatrix} \qquad (16)$$

The measurement covariance matrix $\mathbf{R}$ expresses the inaccuracy of the sensor measurements in rectangular coordinates. The measurement noise is assumed to be zero-mean, white Gaussian with variance σ^2:

$$\mathbf{R} = \begin{pmatrix} \sigma_x^2 & \sigma_{xy}^2 \\ \sigma_{xy}^2 & \sigma_y^2 \end{pmatrix} \qquad (17)$$

The measurements can be transformed from polar sensor coordinates (r, θ) into rectangular sensor coordinates (x, y) by the standard conversion:

$$x = r\cos\theta \qquad (18)$$

$$y = r\sin\theta \qquad (19)$$

The variances in polar coordinates (σ_r^2, σ_θ^2) may be transformed into variances and covariances in rectangular coordinates (σ_x^2, σ_y^2, σ_{xy}^2) by the following equations:

$$\sigma_x^2 = r^2\sigma_\theta^2 \sin^2(\theta) + \sigma_r^2 \cos^2(\theta) \qquad (20)$$

$$\sigma_y^2 = r^2\sigma_\theta^2 \cos^2(\theta) + \sigma_r^2 \sin^2(\theta) \qquad (21)$$

$$\sigma_{xy}^2 = \left(\sigma_r^2 - r^2\sigma_\theta^2\right)\sin\theta\cos\theta \qquad (22)$$

However, according to [16], these transformations only hold if the following conditions are satisfied:

$$\frac{r\sigma_\theta^2}{\sigma_r} < 0.4 \qquad (23)$$

$$\sigma_\theta < 0.4\text{rad} \approx 23° \qquad (24)$$

In the case of the employed SRR sensors, the first condition is only fulfilled for small distances of $r < 3\text{m}$. Thus, the following transformations from polar coordinates into Cartesian coordinates should be used [16]:

$$x = r\cos\theta(1-c) \qquad (25)$$

$$y = r\sin\theta(1-c) \qquad (26)$$

with

$$c = e^{-\sigma_\theta^2} - e^{-\sigma_\theta^2/2} \qquad (27)$$

The corresponding transformations of variances in polar coordinates into variances in rectangular coordinates are as follows:

$$\sigma_x^2 = e^{-2\sigma_\theta^2}[r^2(c_1\cos^2\theta + c_2\sin^2\theta) + \sigma_r^2(c_3\cos^2\theta + c_4\sin^2\theta)] \qquad (28)$$

$$\sigma_y^2 = e^{-2\sigma_\theta^2}[r^2(c_1\sin^2\theta + c_2\cos^2\theta) + \sigma_r^2(c_3\sin^2\theta + c_4\cos^2\theta)] \qquad (29)$$

$$\sigma_{xy}^2 = \sin\theta\cos\theta e^{-4\sigma_\theta^2}\left[\sigma_r^2 + \left(r^2 + \sigma_r^2\right)\left(1 - e^{\sigma_\theta^2}\right)\right] \qquad (30)$$

with

$$c_1 = \cosh 2\sigma_\theta^2 - \cosh\sigma_\theta^2 \qquad (31)$$

$$c_2 = \sinh 2\sigma_\theta^2 - \sinh \sigma_\theta^2 \quad (32)$$

$$c_3 = 2\cosh 2\sigma_\theta^2 - \cosh \sigma_\theta^2 \quad (33)$$

$$c_4 = 2\sinh 2\sigma_\theta^2 - \sinh \sigma_\theta^2 \quad (34)$$

Finally, the measurement matrix **H**, which relates between the measurement vector and the state vector, is given as:

$$\mathbf{H} = \frac{\partial \mathbf{h}(\mathbf{x})}{\partial \mathbf{x}} = \begin{pmatrix} \frac{\partial x}{\partial x} & \frac{\partial x}{\partial v_x} & \frac{\partial x}{\partial y} & \frac{\partial x}{\partial v_y} \\ \frac{\partial y}{\partial x} & \frac{\partial y}{\partial v_x} & \frac{\partial y}{\partial y} & \frac{\partial y}{\partial v_y} \end{pmatrix} = \begin{pmatrix} 1 & 0 & 0 & 0 \\ 0 & 0 & 1 & 0 \end{pmatrix} \quad (35)$$

D. Comparison of MCKF and CMKF

Both the MCKF and the CMKF have been developed for tracking applications where the measurements are obtained in polar coordinates and the state vector is defined in rectangular coordinates. In the case of the MCKF an extended Kalman Filter is used which accommodates the nonlinear coordinate transforms within the measurement matrix, and in the case of the CMKF the nonlinear conversions of measurements and uncertainties are performed by dedicated transformation formulas and thereafter a linear Kalman Filter is employed.

For the given sensor application, a comparison of both approaches shows that the CMKF performs slightly better than the MCKF, especially when the measured distance and bearing values are large while the angular measurement noise is high. Nevertheless, it has to be considered that data association and track management are highly important performance factors as well.

E. Data Association

A Global Nearest Neighbor approach is used to associate new measurements with the existing tracks in polar coordinates. All new measurements within a threshold of σ_r and σ_θ around the predicted relative position of a tracked target are considered to be associated with the track. With the predicted coordinates of the tracked target (r_t , θ_t) and the coordinates of the new measurement (r_m , θ_m) the Mahalanobis distance *d* can be calculated:

$$d = \sqrt{\frac{(r_t - r_m)^2}{\sigma_r^2} + \frac{(\theta_t - \theta_m)^2}{\sigma_\theta^2}} \quad (36)$$

The new measurement with the smallest Mahalanobis distance *d* to the tracked target is finally associated with the track.

F. Ego-Motion-Compensation

The movement of the car is estimated assuming a constant circle movement model of the vehicle. Figure 5 shows a car moving on a circle with radius *r*.

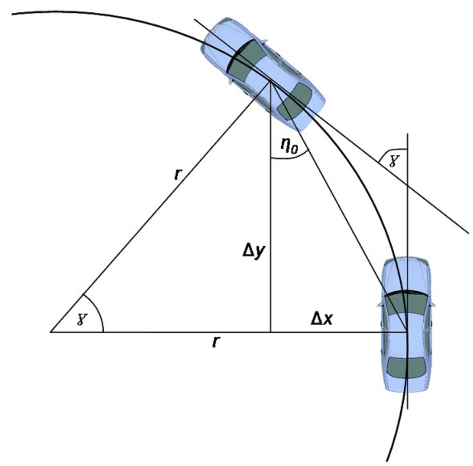

Fig. 5. Car moving on a circle with radius *r*

Given the car velocity v_c , the car acceleration a_c , and the yaw rate ω , the angle of rotation γ of the vehicle around the center of its turning circle can be calculated:

$$\gamma = \frac{1}{r}(v_c T + \frac{1}{2} a_c T^2) \quad (37)$$

with

$$r = \frac{v_c}{\omega} \quad (38)$$

This yields the shift of the coordinate systems Δx and Δy :

Left side of the car: $\Delta x = r - r\cos\gamma$, $\Delta y = r\sin\gamma$

Right side of the car: $\Delta x = -(r - r\cos\gamma)$ (39), $\Delta y = -r\sin\gamma$ (40)

Considering the rotation of the coordinate system, the new relative position of a tracked target (in the Cartesian sensor coordinate system) can be calculated as:

$$x_k = (x_{k-1} - \Delta x)\cos\gamma + (y_{k-1} - \Delta y)\sin\gamma \quad (41)$$

$$y_k = -(x_{k-1} - \Delta x)\sin\gamma + (y_{k-1} - \Delta y)\cos\gamma \quad (42)$$

$$v_{x,k} = v_{x,k-1}\cos\gamma + v_{y,k-1}\sin\gamma \quad (43)$$

$$v_{y,k} = -v_{x,k-1}\sin\gamma + v_{y,k-1}\cos\gamma \quad (44)$$

V. Sensor Data Fusion

The single-sensor-tracked-targets obtained from all sensors belonging to the same array are integrated by homogeneous sensor data fusion. For this purpose, a gate is defined for each single-sensor-tracked-target. The gate is modeled as an ellipse around the relative position of the single-sensor-tracked-target (x_t , y_t):

$$\frac{(x - x_t)^2}{a^2} + \frac{(y - y_t)^2}{b^2} = 1 \quad (45)$$

The values for σ_x and σ_y within the state covariance matrix **P** define the lengths of the major axis a and the minor axis b of the ellipse:

$$a = 3\sqrt{\sigma_x^2} \quad (46)$$

$$b = 3\sqrt{\sigma_y^2} \quad (47)$$

Whenever the gates of $n \geq 2$ single-sensor-tracked-targets intersect, the n single-sensor-tracked-targets are associated with each other and merged to an integrated target $\mathbf{x}_{\text{int}}$. The weighted average of relative position and relative velocity is calculated, using the accuracy as weighting factor:

$$x_{\text{int}} = \frac{\sum_{i=1}^{n} \frac{1}{\sigma_{x,i}} x_i}{\sum_{i=1}^{n} \frac{1}{\sigma_{x,i}}} \tag{48}$$

$$y_{\text{int}} = \frac{\sum_{i=1}^{n} \frac{1}{\sigma_{y,i}} y_i}{\sum_{i=1}^{n} \frac{1}{\sigma_{y,i}}} \tag{49}$$

$$v_{x,\text{int}} = \frac{\sum_{i=1}^{n} \frac{1}{\sigma_{v_x,i}} v_{x,i}}{\sum_{i=1}^{n} \frac{1}{\sigma_{v_x,i}}} \tag{50}$$

$$v_{y,\text{int}} = \frac{\sum_{i=1}^{n} \frac{1}{\sigma_{v_y,i}} v_{y,i}}{\sum_{i=1}^{n} \frac{1}{\sigma_{v_y,i}}} \tag{51}$$

The elements of the weighted state error covariance matrix $\mathbf{P}_{\text{int}}(k,l)$ are computed accordingly:

$$\mathbf{P}_{\text{int}}(k,l) = \frac{1}{\sum_{i=1}^{n} \frac{1}{\mathbf{P}(k,l)_i}} \tag{52}$$

VI. Multi-Sensor-Multi-Target-Tracking

Based on the integrated targets, multi-sensor-multi-target-tracking is achieved by applying a linear Kalman Filter. For this purpose, the approach of single-sensor-multi-target-tracking is adapted.

A Global Nearest Neighbor approach is used to associate new integrated targets with the existing tracks in rectangular coordinates. All new integrated targets within a threshold of σ_x and σ_y around the predicted relative position of a tracked integrated target are considered to be associated with the track. With the predicted coordinates of the tracked integrated target (x_t , y_t) and the coordinates of the new integrated target (x_{int} , y_{int}) the statistical distance d is calculated:

$$d = \sqrt{\frac{(x_t - x_{\text{int}})^2}{\sigma_x^2} + \frac{(y_t - y_{\text{int}})^2}{\sigma_y^2}} \tag{53}$$

The new integrated target with the smallest statistical distance d to the tracked integrated target is finally associated with the track.

The ego-motion-compensation described in Section IV for single-sensor-multi-target-tracking is applied for multi-sensor-multi-target-tracking accordingly.

VII. Experimental Results

A typical LCW scenario is illustrated in Figure 6. The multi-sensor-tracked-targets (circles) obtained from a parallel driving vehicle in a corresponding real road traffic situation are shown in Figure 7. It should be noted that in this experiment the ego-vehicle was equipped with four SRR sensors on each side for test purposes. In Figure 7 it can be observed that the distances of the four nearest multi-sensor-tracked targets from the side of the ego-vehicle are approximately 0.5m. These targets represent tracked reflection points on the boundary of the parallel driving vehicle. The other multi-sensor-trackedtargets are either caused by further distant reflection points on the target-vehicle or by multiple reflections between the surface of the target-vehicle and the surface of the ego-vehicle.

Fig. 6. LCW scenario

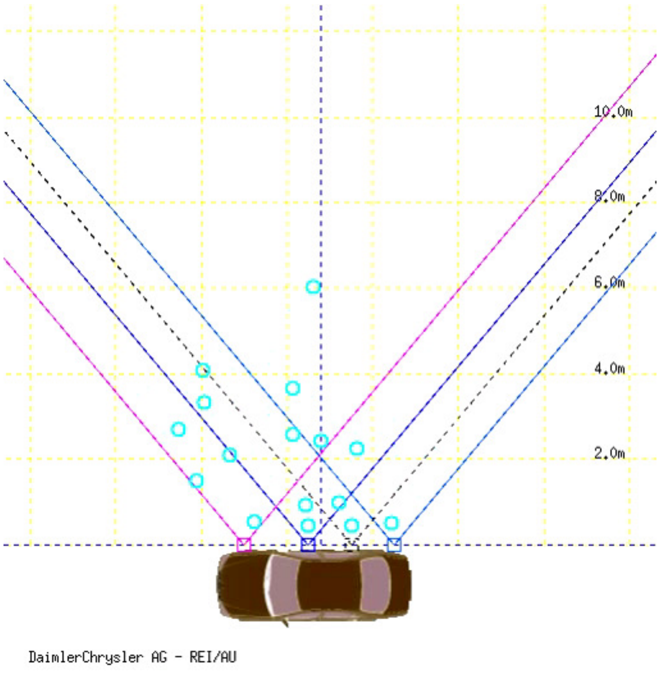

Fig. 7. Multi-sensor-tracked-targets (circles) obtained in real road traffic

The multi-sensor-tracked-targets are parameterized by their relative positions, relative velocities, measures of quality, measurement covariance matrices, and target identifiers. The most relevant multi-sensor-tracked-targets on each side of the ego-vehicle are identified in order to be provided to the LCW function. For determining the relevance of tracked targets, their relative positions and relative velocities are considered and the time-to-collision is calculated.

An optical and acoustical LCW signal is activated when either the calculated time to collision or the distance of a multi-sensor-tracked-target from the side of the ego-vehicle falls below a respective threshold, while the thresholds are adapted by the speed of the ego-vehicle.

VIII. Conclusion

Signal processing algorithms for the implementation of a lateral collision warning function have been developed. The raw sensor measurements are filtered and single-sensor-multi-target-tracking is realized for each sensor independently by applying a Mixed Coordinates Kalman Filter (MCKF) and a Converted Measurement Kalman Filter (CMKF) alternatively. A comparison of both approaches shows that the CMKF performs slightly better than the MCKF, especially when the measured distance and bearing values are large while the angular measurement noise is high.

The single-sensor-tracked-targets obtained from all sensors belonging to the same array are integrated by homogeneous sensor data fusion. This process involves gating according to the given uncertainties. Whenever the gates of single-sensor-tracked-targets intersect, the single-sensor-tracked-targets are associated with each other and merged to an integrated target. The weighted average of relative position and relative velocity is calculated, using the accuracy as weighting factor.

Based on the integrated targets, multi-sensor-multi-target-tracking is achieved by applying a linear Kalman Filter. The Global Nearest Neighbor approach is used to associate new integrated targets with existing tracks. For the implementation of the Kalman Filter, a constant velocity model is chosen.

References

[1] Y. Bar-Shalom, "Tracking Methods in a Multitarget Environment" *IEEE Transactions on Automatic Control*, Vol. 23, No. 4, pp. 618–626, 1978.

[2] Y. Bar-Shalom and T. Fortmann, *Tracking and Data Association*. San Diego: Academic Press, 1988.

[3] Y. Bar-Shalom (Editor), *Multitarget-Multisensor Tracking: Advanced Applications*. Vol. I, Boston: Artech House, 1990.

[4] Y. Bar-Shalom (Editor), *Multitarget-Multisensor Tracking: Applications and Advances*. Vol. II, Boston: Artech House, 1992.

[5] Y. Bar-Shalom and X. R. Li, *Estimation and Tracking: Principles, Techniques, and Software*. Boston: Artech House, 1993.

[6] Y. Bar-Shalom, X. R. Li, and T. Kirubarajan, *Estimation with Applications to Tracking and Navigation: Theory, Algorithms, and Software for Information Extraction*. New York: John Wiley & Sons, 2001.

[7] S. S. Blackman, *Multiple-Target Tracking with Radar Applications*. Boston: Artech House, 1986.

[8] S. S. Blackman and R. Popoli, *Design and Analysis of Modern Tracking Systems*. Boston: Artech House, 1999.

[9] I. Gresham, A. Jenkins, R. Egri, C. Eswarappa, N. Kinayman, N. Jain, R. Anderson, F. Kolak, R. Wohlert, S. P. Bawell, J. Bennett, and J.-P. Lanteri, "Ultra-Wideband Radar Sensors for Short-Range Vehicular Applications" *IEEE Transactions on Microwave Theory and Techniques*, Vol. 52, No. 9, pp. 2105–2122, 2004.

[10] D. L. Hall and J. Llinas (Editors), *Handbook of Multisensor Data Fusion*. Boca Raton: CRC Press, 2001.

[11] S. J. Julier and J. K. Uhlmann, "A New Extension of the Kalman Filter to Nonlinear Systems", in *Proceedings of AeroSense: The 11th Annual International Symposium on Aerospace/Defense Sensing, Simulation, and Controls*, Orlando, pp. 182–193, 1997.

[12] S. J. Julier and J. K. Uhlmann, "Reduced Sigma Point Filters for the Propagation of Means and Covariances Through Nonlinear Transformations", in *Proceedings of the 2002 American Control Conference*, Anchorage, pp. 887–892, 2002.

[13] R. E. Kalman, "A New Approach to Linear Filtering and Prediction Problems" *Transactions of the ASME – Journal of Basic Engineering*, Series D, Vol. 82, pp. 35–45, 1960.

[14] R. E. Kalman and R. S. Bucy, "New Results in Linear Filtering and Prediction Theory" *Transactions of the ASME – Journal of Basic Engineering*, Series D, Vol. 83, pp. 95–108, 1961.

[15] T. Lefebvre, H. Bruyninckx, and J. De Schutter, "Kalman filters for non-linear systems: a comparison of performance" *International Journal of Control*, Vol. 77, No. 7, pp. 639–653, 2004.

[16] D. Lerro and Y. Bar-Shalom, "Tracking With Debiased Consistent Converted Measurements Versus EKF" *IEEE Transactions on Aerospace and Electronic Systems*, Vol. 29, No. 3, pp. 1015–1022, 1993.

[17] P. S. Maybeck, *Stochastic models, estimation, and control*. Vol. 1-3, New York: Academic Press, 1979.

[18] A. Polychronopoulos, N. Floudas, A. Amditis, D. Bank, and B. van den Broek, "Data fusion in multi sensor platforms for wide-area perception", in *Proceedings of the IEEE Intelligent Vehicles Symposium*, Tokyo, pp. 412–417, 2006.